

Deformation, Strain Rate Sensitivity and Activation Volume of Ultrafine-grained Commercially Pure Ti

Liu Xiaoyan¹, Zhang Qi¹, Yang Xirong¹, He Xiaomei¹, Kang Shumei², Gao Feilong¹

¹ Xi'an University of Architecture and Technology, Xi'an 710055, China; ² University of Science and Technology Liaoning, Anshan 114051, China

Abstract: The deformation behavior of ultrafine-grained (UFG) commercially pure (CP) Ti was investigated. The strain rate sensitivity and activation volume were calculated based on strain rate jump tests performed at a temperature range of 250–450 °C and a strain rate of $1 \times 10^{-4} \sim 1 \text{ s}^{-1}$. The results show that flow softening effect occurs in steady state of deformation of UFG CP Ti, which is controlled by high-angle grain boundaries and dislocation activity during the deformation process. Strain rate sensitivity of UFG CP Ti is relatively low in value and increases with the rise of temperature. The activation volume of UFG CP Ti is also low in value but invariant with temperature. The values of strain rate sensitivity and activation volume indicate that dislocation-dislocation interactions within the grain interiors take place scarcely and interactions between dislocation and grain boundary can significantly affect plastic deformation of UFG CP Ti.

Key words: ultrafine-grained; commercially pure Ti; strain rate sensitivity; activation volume; flow softening

Polycrystalline materials with ultrafine-grained (UFG) or nano-crystalline (NC) structures have received enormous scientific attention due to their unusual mechanical properties^[1-5]. The UFG and NC materials processed by severe plastic deformation (SPD) techniques are distinguished by high dislocation density and non-equilibrium grain boundaries, which lead to the inhomogeneous deformation behaviors^[6]. Extensive research has been performed for understanding the deformation behavior of UFG and NC materials, such as Cu, Al, Ti and their alloys^[7-16]. It is found that in UFG Al, the deformation mechanism is operated by the dislocation interactions in the higher strain rate range, while in the lower strain rate range it is related to grain boundary sliding^[8]. The deformation of UFG Ti and its alloys are also strongly dependent on strain rate and temperature^[10,11,13]. The flow stress curves of TiBw/TA15 composite are very sensitive to strain rate: flow curves exhibit typical work hardening features at high strain rate and substantial flow softening occurs at low strain rate^[15]. Moreover, the strain rate sensitivity and activation volume are strongly dependent on

grain size. Increase in the strain rate sensitivity and decrease in the activation volume of Cu and Ti are measured with decreasing the grain size^[14,17]. However, the contradictory result was reported that the strain rate sensitivity of UFG Ti drops by a factor of 2–3 relative to that for coarse grained (CG) Ti^[10]. By analyzing the strain rate sensitivity values, the apparent activation energy and the microstructure evolution, it can be inferred that grain boundary sliding in the fine-grained TA15 alloy is accommodated by grain boundary diffusion at high temperatures and low strain rates, but grain boundary sliding is accommodated by dislocation glide creep at low temperatures and high strain rates^[16].

There is a transition from strengthening to softening by high-angle grain boundaries in steady state of deformation of UFG Cu, which is in terms of generation and grain boundary diffusion controlled annihilation of lattice dislocations at grain boundaries^[7]. Long et al^[11] found that UFG Ti also shows a clear stage of strain softening, while the inverse trend has been reported that the steady state deformation resistance of CG and UFG Ti is not significantly different^[12]. Therefore, in this

Received date: June 26, 2019

Foundation item: National Natural Science Foundation of China (51474170); Nature Science Foundation of Shaanxi Province (2016JQ5026); Research Fund of Educational Commission of Liaoning Province (2017LNQN14)

Corresponding author: Liu Xiaoyan, Ph. D., Associate Professor, School of Metallurgical Engineering, Xi'an University of Architecture and Technology, Xi'an 710055, P. R. China, Tel: 0086-29-82202937, E-mail: liuxiaoyan@xauat.edu.cn

Copyright © 2020, Northwest Institute for Nonferrous Metal Research. Published by Science Press. All rights reserved.

work, deformation behavior and deformation mechanisms of UFG CP Ti were analyzed using two activation parameters, i.e. strain rate sensitivity and activation volume by compression strain rate jump tests.

1 Experiment

CG and UFG CP Ti were prepared from the same batch of materials with a chemical composition of 0.012 wt% Fe, 0.022 wt% C, 0.003 wt% N, 0.001 wt% H, 0.06 wt% O and balance Ti (grade I). The UFG CP Ti was fabricated by equal channel angular pressing (ECAP) up to 4 passes via route C at room temperature using a 90° die, resulting in the cumulative equivalent strain of 4. In the ECAP via route C, the billet was rotated 180° clockwise along its longitudinal axis between adjacent passes^[18]. The detailed characterization of microstructures of CG and UFG CP Ti can be found in Ref.[19]. Here the most important features were described. The average grain size of CG CP Ti was about 25 μm. A homogenous microstructure was obtained, which was characterized by equiaxed grains/subgrains with an average grain size of about 150 nm after 4 passes. The grain boundary character distribution determined by EBSD is shown in Fig.1. It can be seen that there is a high fraction of high-angle grain boundaries (HAGBs, ~88%) in CG CP Ti (0P). The fraction of HAGBs in UFG CP Ti firstly decreases with increasing the number of ECAP, and then increases to 55% after 4 passes.

The cylindrical specimens with a diameter of 6 mm and a length of 9 mm of CG and UFG CP Ti were uniaxially compressed on a Gleeble-3500 simulator machine in the temperature range of 250~450 °C and strain rate of $1 \times 10^{-4} \sim 1 \text{ s}^{-1}$. The compression direction of UFG CP Ti was oriented parallel to the ECAP axis. Molybdenum disulphide-graphite paste was used as lubricant. The load-displacement data were obtained from the compression tests and then converted to true stress-true strain curves using standard equations.

2 Results and Discussion

2.1 True stress-true strain curves

Fig.2 presents the true stress-true strain curves of CG and

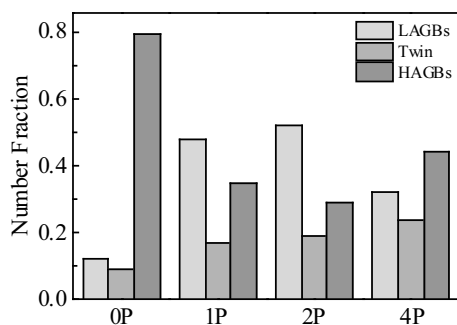


Fig.1 Grain boundary character distribution for CP Ti processed by ECAP for different passes 0P-4P at room temperature

UFG CP Ti at different temperatures with the strain rate of $1 \times 10^{-4} \text{ s}^{-1}$. It is observed that the mechanical behavior of UFG CP Ti considerably differs from that of CG CP Ti. The flow stress of UFG CP Ti reaches the peak stress at a relatively small strain and goes into a steady state. The high work hardening rate at the onset of the plastic deformation in UFG CP Ti is due to the fine grain structure and high density of dislocation after ECAP. The decrease of work hardening rate of UFG CP Ti can be attributed to the increase of dynamic recovery/recrystallization and probable grain coarsening^[13]. The higher the temperature, the more remarkable the strain softening. In contrast, the flow stress of CG CP Ti generally shows an extended range of work hardening after yielding. Work hardening rate of CG CP Ti decreases and falls to zero at peak stress with increasing the temperature and true strain. The difference in work hardening rate of CG and UFG CP Ti can also be found in the strain value (marked by the black square in Fig.2) corresponding to the same flow stress of two materials. These strain values (0.693, 0.578 and 0.237) gradually decrease with increasing the temperature. The flow stress of UFG CP Ti is lower than that of CG CP Ti during the whole deformation process at 450 °C. It means that the strain softening effect of UFG CP Ti is more significant than that of CG counterpart, which is different with the result of Blum et al^[12].

The yield strength of CG and UFG CP Ti at different temperatures with the strain rate of $1 \times 10^{-4} \text{ s}^{-1}$ is exhibited in Fig.3. It is noted that the yield strength of UFG CP Ti is higher than that of CG counterpart as the temperature is lower than the recrystallization temperature (250, 350 and 400 °C). The decrease in yield strength of UFG CP Ti is larger than that of CG CP Ti at the same temperature. However, the yield strength of UFG CP Ti is lower than that of CG counterpart as the temperature exceeds the recrystallization temperature (450 °C). There is a transition from strengthening to softening in yield strength for UFG CP Ti. The first effect can be explained by the strong work hardening related with ECAP. The second one may be explained by the growth of subgrain and softening effect caused by high-angle grain boundaries in UFG CP Ti at the higher temperature. The negligible strain hardening behavior of UFG CP Ti is mainly due to dynamic recovery or enhancing dislocation annihilation process.

2.2 Strain rate sensitivity and activation volume

The strain rate sensitivity of flow stress is determined by the strain rate jump tests. The strain rate sensitivity exponent, m , is defined as follows:

$$m = \left(\frac{\partial \ln \sigma}{\partial \ln \dot{\epsilon}} \right)_{\epsilon, T} \approx \left(\frac{\Delta \ln \sigma}{\Delta \ln \dot{\epsilon}} \right)_{\epsilon, T} \approx \frac{\ln(\sigma_2 / \sigma_1)}{\ln(\dot{\epsilon}_2 / \dot{\epsilon}_1)} \quad (1)$$

In addition, the strain rate sensitivity can be understood by relating to the activation volume v ^[20]:

$$m = \frac{\sqrt{3}kT}{\sigma v} \quad (2)$$

where k is the Boltzmann constant ($k=1.38 \times 10^{-23} \text{ J} \cdot \text{K}^{-1}$), and T

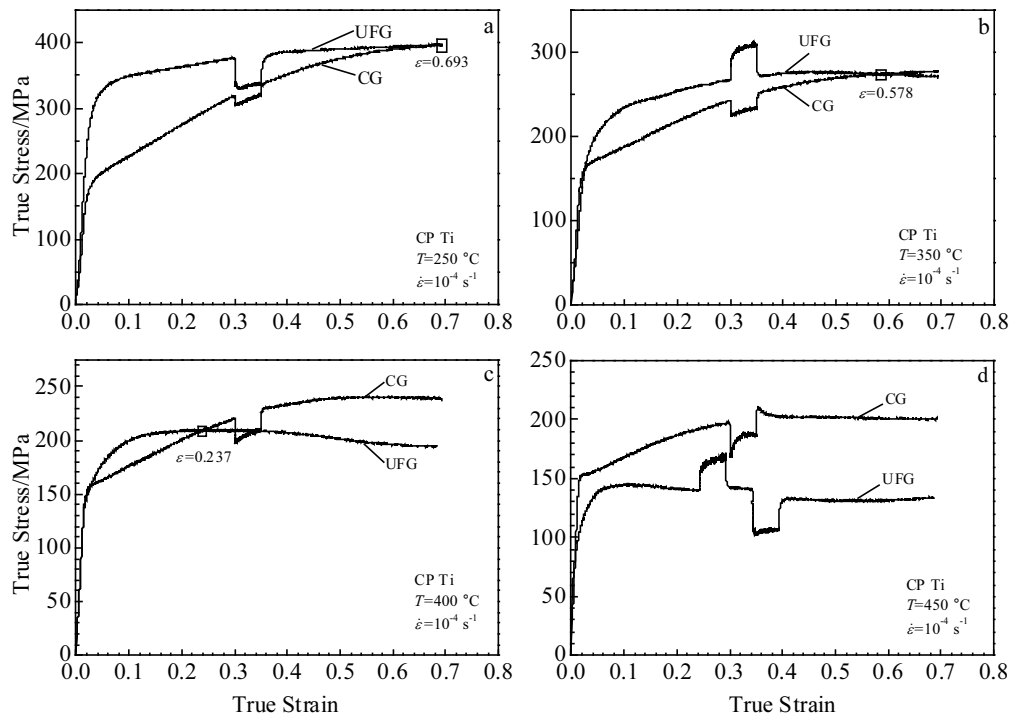


Fig.2 True stress-strain curves of CG and UFG CP Ti at different temperatures with the strain rate of 10^{-4} s^{-1} : (a) 250 °C, (b) 350 °C, (c) 400 °C, and (d) 450 °C

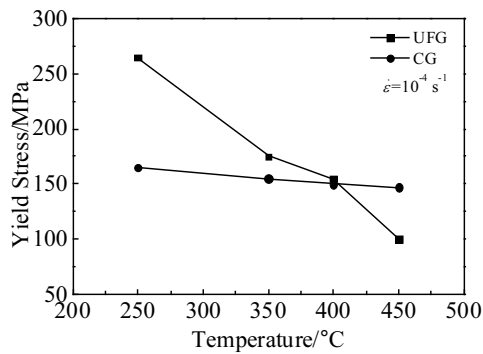


Fig.3 Yield stress of CG and UFG CP Ti at different temperatures with strain rate of 10^{-4} s^{-1}

is the absolute temperature. Fig.4 shows the dependence of strain rate sensitivity m and activation volume v on temperature and grain size. It can be seen from Fig.4a that the strain rate sensitivity m of both CG and UFG CP Ti increases with increasing the temperature. The strain rate sensitivity m increases with decreasing the grain size, especially at higher temperature (450 °C). In other words, a distinct dependence of m with T is typical for UFG CP Ti, while such dependence is very slight for CG CP Ti. The m values of CG and UFG CP Ti are in the range of 0.022~0.041 and 0.033~0.120, respectively. The dependence of strain rate sensitivity on the grain size in present work shows the similar trend with hexagonal

close-packed (hcp) metals reported in Ref.[14,21]. The dependence of activation volume on grain size and temperature is plotted in Fig.4b. The activation volume is expressed as b^3 , where b is the Burger's vector of the prefer slip system $\{10\bar{1}0\} \langle 11\bar{2}0 \rangle$ for titanium, $b=2.95 \times 10^{-10} \text{ m}$. The values of activation volume are calculated to be in the range of $100b^3 \sim 135b^3$ and $30b^3 \sim 57b^3$ by jump tests for CG and UFG CP Ti, respectively. It can be seen from Fig.4b that the activation volume is strongly dependent on grain size and decreases with decreasing the grain size. However, the activation volume is independent on temperature at the same strain rate.

Generally, as the grain size decreases from micrometers to ultrafine or nanoscale, the plastic deformation mechanism may be changed from dislocation slip inside the grains to grain boundary related process such as grain boundary sliding or Coble creep. The value of strain rate sensitivity is expected to be 0.5 or 1.0 when the plastic deformation is controlled entirely by grain boundary sliding or Coble creep^[22], respectively. However, the maximum value of strain rate sensitivity for UFG CP Ti in this work is calculated to be 0.12, which is much smaller than the value mentioned above. In addition, the minus activation volume ($30b^3$) is still much larger than the value for grain boundary dominated process such as diffusion of vacancy involved in the exchange between the vacancy and lattice atom ($\sim b^3$). Such values have seldom been observed for UFG or NC hcp metals processed by SPD although the activation volume decreases with decreasing the grain size and

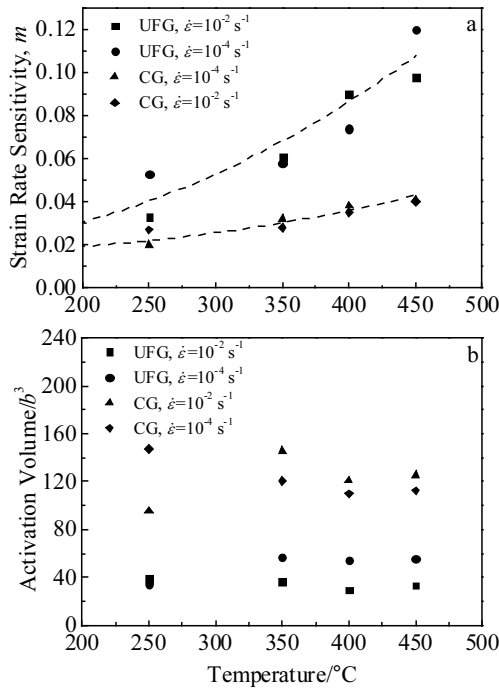


Fig.4 Strain rate sensitivity (a) and activation volume (b) of CG and UFG CP Ti at different temperatures and strain rates

increasing the strain^[23,24]. Therefore, the grain boundary controlled process, such as grain boundary sliding or atomic diffusion mechanism can be ruled out for UFG CP Ti. For CG and UFG CP Ti, in general, forest dislocation is the primary short-range barriers to plastic deformation. The dislocation-dislocation interaction within the grains is the main plastic deformation mechanism for CG CP Ti, while the activation volume is relatively low for UFG CP Ti, suggesting that dislocation-dislocation interactions inside the grain take place scarcely. The increase in strain rate sensitivity and decrease in activation volume of UFG CP Ti are necessarily related to the non-equilibrium high-angle grain boundaries, which are typical microstructures of UFG materials fabricated by SPD. Wang^[25,26] and Dalla Torre^[27] reported that the activation volume of NC fcc materials is in the range of $10b^3 \sim 50b^3$ and suggested that the thermal obstacles to dislocation slip are resulted from the interaction of the dislocations and grain boundaries. Milligan^[28] presented that the dislocation sources are no longer inside the grains, but grain boundaries act as both sources and sinks for dislocations in the bulk UFG or NC materials. Dislocations are generated within grain boundaries, glide quickly across the grains and are absorbed into the opposite grain boundaries. This scenario is built in part on the results of molecular dynamics simulations of NC Al^[29]. The number of active slip systems in hcp Ti is expected to be lower than in the cubic system, making the grain boundary source-sink concept even more attractive for UFG CP Ti. The low activation volume and high strain rate sensitivities obtained

from the present work support the notion that high-angle grain boundaries act as sources and sinks for dislocations, which contributes to plastic deformation in UFG CP Ti.

2.3 Softening effect in steady state of deformation

There is an extended range of strain softening for UFG CP Ti in contrast to the work hardening in CG CP Ti.

The steady state subgrain size w is closely related to the stress:

$$\omega_{\infty,CG} = k_{\omega} \frac{bG}{\sigma} \quad (3)$$

where k_{ω} is a numerical factor between 10 and 30^[30,31], $k_{\omega}=10$ for Ti and Ti alloys^[12]; G is the elastic shear modulus, $G=45$ GPa for pure Ti^[32]; b is the length of the Burger's vector for titanium.

Fig.5 shows the initial grain size of CG and UFG CP Ti in relation to the steady state subgrain size according to Eq.(3). Shape horizontal bands display the initial values of grain size d_0 for CG and UFG CP Ti. The initial grain sizes of CG and UFG CP Ti are determined to be $d_{0,CG}=25 \mu\text{m}$ and $d_{0,UFG}=150$ nm according to Ref.[19]. The initial subgrain size is not exactly known. Zhu et al^[33] reported that subgrains contain dislocations, but no dislocation cells are in the size range of 60~150 nm and subgrains smaller than 100 nm may not contain any dislocations except at their boundary in the nano-structured Ti. By definition of w , the spacing of high-angle grain boundaries d is an upper limit of the size of subgrains to be formed in the course of plastic deformation. The dotted vertical lines shown in Fig.5 mark the condition for subgrain

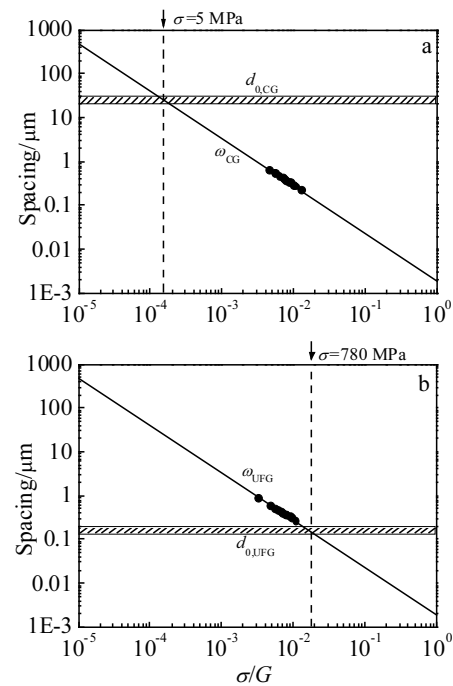


Fig.5 Subgrain size of deformed CG (a) and UFG (b) CP Ti as a function of shear modulus normalized stress

formation, $d_{0,CG}=w_{\infty,CG}=10bG/\sigma$. This means that no new subgrains may be formed in CG and UFG CP Ti when the stress is lower than 5 and 780 MPa, respectively. The steady state subgrains size of CG and UFG CP Ti formed during deformation can be calculated according to Eq.(3) from experimental maximum flow stress, marked by black circles in Fig.5. It can be seen from Fig.5a that each deformed grain is subdivided into the subgrains with different sizes for CG CP Ti during the deformation process. The flow stress of CG CP Ti is dependent on the subgrain boundaries instead of high-angle grain boundaries during the deformation process.

However, no new subgrains may be formed in UFG CP Ti due to $d_{0,UFG}<w_{\infty}$. Grains are much smaller than the dislocation mean free length of Ti. Therefore, dislocation activities can not be developed in the same manner for UFG CP Ti, as demonstrated by molecular dynamic (MD) simulations^[34]. The mean free path of dislocations is no longer determined by the dislocation structure, but limited by the high-angle grain boundaries. Fewer dislocations are stored inside the grains and more dislocations are stored at the high-angle grain boundaries. Hayes et al^[35] reported that high-angle grain boundaries act as sources and sinks for dislocations in the bulk UFG or NC materials. Thus the materials are softened by the reduction of dislocation density in the steady state. The removal of subgrain boundaries with the grains as obstacles to dislocation motion and easy annihilation of lattice dislocations at high-angle grain boundaries under the condition of $d_{0,UFG}<w_{\infty}$ are able to explain the softening discussed above. The microstructure observation of deformed specimen by TEM shows that the maximum grain size available at 450 °C is still below 1 μm ^[13]. Therefore, the major process occurring during deformation at elevated temperatures is subgrain growth from $w_{0,UFG}$ up to $d_{0,UFG}$. The boundary controlled dislocation activities may therefore also contribute to the increase of strain rate sensitivity and much reduced activation volume for ultrafine-grained metals^[26]. High-angle grain boundaries may soften materials in the steady state of deformation by enhancing the annihilation of dislocations^[35].

3 Conclusions

1) The flow stress of UFG CP Ti exhibits a steady state, while the flow stress of CG CP Ti increases monotonically. The flow stress of UFG CP Ti is lower than that of CG CP Ti as the temperature is above the recrystallization temperature. High-angle grain boundaries in UFG CP Ti may soften materials in the steady state of deformation by enhancing the annihilation of dislocations.

2) The strain rate sensitivity and activation volume are strongly dependent on the grain size. With decreasing the grain size, the strain rate sensitivity increases while the activation volume decreases. High strain rate sensitivity (0.033~0.120) and low activation volume ($30b^3\sim 57b^3$) demonstrate that the interactions between dislocation and

grain boundary can be considered as a possible plastic deformation mechanism for UFG CP Ti.

References

- 1 Choi I C, Kim Y J, Wang Y M et al. *Acta Materialia*[J], 2013, 61: 7313
- 2 Muñoz J A. *Materials Letters*[J], 2019, 238: 42
- 3 Niehuesbernd J, Bruder E, Müller C. *Materials Science and Engineering A*[J], 2018, 711:325
- 4 Afifi M A, Wang Y C, Henrique P et al. *Journal of Alloys and Compounds*[J], 2018, 769: 631
- 5 Cabibbo M, Paoletti C, Minárik P et al. *Materials Letters*[J], 2019, 237: 5
- 6 Zhu Y T, Langdon T G. *Materials Science and Engineering A*[J], 2005, 409: 234
- 7 Li Y J, Zeng X H, Blum W. *Acta Materialia*[J], 2004, 52: 5009
- 8 Wang M L, Shan A D. *Journal of Alloys and Compounds*[J], 2008, 455: 10
- 9 Sabirov I, Barnett M R, Estrin Y et al. *Scripta Materialia*[J], 2009, 61: 181
- 10 Jia D, Wang Y M, Ramesh K T et al. *Applied Physics Letters*[J], 2001, 79(5): 611
- 11 Long F W, Jiang Q W, Xiao L et al. *Materials Transactions*[J], 2011, 52: 1617
- 12 Blum W, Li Y J, Breutinger F. *Materials Science and Engineering A*[J], 2006, 462: 275
- 13 Liu X Y, Zhao X C, Yang X R et al. *Advanced Engineering Materials*[J], 2014, 16: 371
- 14 Wang F, Li B, Gao T T et al. *Surface and Coating Technology*[J], 2013, 228: 254
- 15 Zhang R, Wang D J, Huang L J et al. *Journal of Alloys and Compounds*[J], 2017, 722: 970
- 16 Sun Q J, Wang G C. *Materials Science and Engineering A*[J], 2014, 606: 401
- 17 Dalla Torre F H, Pereloma E V, Davies C H J. *Scripta Materialia*[J], 2004, 51: 367
- 18 Liu X Y, Zhao X C, Yang X R et al. *Advanced Engineering Materials*[J], 2014, 16: 371
- 19 Zhao X C, Yang X R, Liu X Y et al. *Materials Science and Engineering A*[J], 2014, 607: 482
- 20 Meyers M A, Chawla K K. *Mechanical Metallurgy*[M]. New Jersey: Prentice Hall, 1984
- 21 Chui H J, Kim Y, Shin J H et al. *Materials Science and Engineering A*[J], 2010, 527: 1565
- 22 Ashby M F, Verrall R A. *Acta Metallurgica*[J], 1973, 21: 149
- 23 Conrad H, Narayan J. *Acta Materialia*[J], 2002, 50: 5067
- 24 Conrad H, Narayan J. *Scripta Materialia*[J], 2000, 42: 1025
- 25 Wang Y M, Ma E. *Materials Science and Engineering A*[J], 2004, 375-377: 46
- 26 Wang Y M, Hamza A V, Ma E. *Acta Materialia*[J], 2006, 54: 2715
- 27 Dalla Torre F H, Swygenhoven H V, Victoria M. *Acta Materialia* [J], 2002, 50: 3957
- 28 Milligan W W. *Interfacial and Nanoscale Fracture*[C].

- Amsterdam: Pergamon Press, 2003
- 29 Yamakov V, Wolf D, Salazar M et al. *Acta Materialia*[J], 2001, 49: 2713
- 30 Raj S V, Pharr G. *Materials Science and Engineering A*[J], 1986, 81: 217
- 31 Blum W, Straub S, Vogler S. *Proceedings of the 9th International Conference on the Strength of Metals and Alloys*[C]. London: Freund Publishing House, 1991
- 32 Frost H J, Ashby M F. *Deformation Mechanism Maps*[M]. Oxford: Pergamon Press, 1982
- 33 Zhu Y T, Huang J Y, Gubicza J et al. *Journal of Materials Research*[J], 2003, 18: 1908
- 34 Hasnaoui A, Derlet P M, Swygenhoven H V. *Acta Materialia*[J], 2004, 52: 2251
- 35 Hayes R W, Witkin D, Zhou F et al. *Acta Materialia*[J], 2004, 52: 4259

超细晶工业纯钛的变形、应变速率敏感性和激活体积

刘晓燕¹, 张琪¹, 杨西荣¹, 何晓梅¹, 亢淑梅², 高飞龙¹

(1. 西安建筑科技大学, 陕西 西安 710055)

(2. 辽宁科技大学, 辽宁 鞍山 114051)

摘要: 在温度为 250~450 °C、应变速率为 $1 \times 10^{-4} \sim 1 \text{ s}^{-1}$ 的条件下, 对超细晶工业纯钛进行变速率压缩实验, 计算超细晶工业纯钛的应变速率敏感性因子和激活体积, 并研究超细晶工业纯钛的变形行为。结果表明: 超细晶工业纯钛在稳态变形阶段存在流变软化效应, 这是受变形过程中大角度晶界和位错活动所控制的。超细晶工业纯钛的应变速率敏感性因子和激活体积在数值上都相对较低, 应变速率敏感性随着变形温度的升高而增加, 但激活体积独立于变形温度。应变速率敏感性和激活体积的数值表明晶粒内部位错之间几乎无交互作用, 而位错与晶界之间的交互作用显著影响超细晶工业纯钛的塑性变形。

关键词: 超细晶; 工业纯钛; 应变速率敏感性; 激活体积; 流变软化

作者简介: 刘晓燕, 女, 1980 年生, 博士, 副教授, 西安建筑科技大学冶金工程学院, 陕西 西安 710055, 电话: 029-82202923, E-mail: liuxiaoyan@xauat.edu.cn